

## Analytical study on effects of fracture energy for crack propagation in arch dam during large earthquake

H. Sato, M. Kondo & T. Sasaki

*National Institute Land and Infrastructure Management, Tsukuba, Japan*

H. Hiramatsu

*Eight-Japan Engineering Consultants Inc., Osaka, Japan*

H. Kojima

*CTI Engineering Co., Ltd., Tokyo, Japan*

**ABSTRACT:** In the seismic performance evaluation of concrete dams against large scale earthquakes, crack propagation analysis based on smeared crack model is sometimes performed as a method of nonlinear dynamic analysis to estimate damage process. But it is not easy to set some parameters required for the analysis appropriately, such as fracture energy which is one of the physical properties related to fracture characteristics of dam concrete, due to shortage of the number of full scale experimental tests. In this paper, we reviewed related past experimental studies including static and rapid wedge splitting tests with comparatively large fracture energy, and conducted analytical studies on the effects of difference in fracture energy for crack propagation in a concrete arch dam considering such experimental results data. The results showed that the fracture energy had an important influence on crack distributions and cracks in dam body were localized as fracture energy increased.

**RÉSUMÉ:** Dans l'évaluation des performances sismiques des barrages en béton soumis à de forts séismes, l'analyse de la propagation des fissures basée sur un modèle de fissure diffuse est parfois utilisée comme méthode d'analyse dynamique non linéaire pour estimer le processus d'endommagement. Mais, il n'est pas facile de fournir certains paramètres nécessaires à l'analyse, tels que l'énergie de fracturation, qui est l'une des propriétés physiques liées aux caractéristiques de rupture du béton du barrage en raison du nombre insuffisant d'essais expérimentaux à pleine grandeur. Dans cet article, nous avons examiné des études expérimentales antérieures pertinentes, y compris des essais de fissuration en coin statique et rapide avec une énergie de fracturation relativement grande, et réalisé des études analytiques sur les effets de la différence d'énergie de fracturation sur la propagation des fissures dans les barrages-poids et les barrages-voûtes en béton en tenant compte des résultats de ces données expérimentales. Les résultats ont montré que l'énergie de fracturation avait une influence importante sur la distribution des fissures et que les fissures dans le corps du barrage étaient localisées à mesure que l'énergie de fracturation augmentait.

### 1 INTRODUCTION

To evaluate seismic performance of concrete dams during large earthquakes, crack propagation analysis is sometimes conducted, and it is necessary to appropriately set various parameters to accurately estimate damaged area. However, in some cases, it is not easy to appropriately set some parameters such as damping ratio when the strong acceleration record has not obtained at the dam. It is also difficult to set the value of fracture energy because there are few test cases for dam concrete. Therefore, in this paper, for the purpose of grasping

fundamental effects of fracture energy, basic analytical investigation was conducted on the influence of the fracture energy on the crack propagation analysis.

Fracture energy of dam concrete is a particularly important parameter among the input physical properties required for evaluating crack growth of concrete dams. The value is obtained from the fracture energy laboratory tests including wedge splitting tests, but there are few test cases for dam concrete using the maximum aggregate size of 80 to 150 mm. For this reason, we first conducted literature search to investigate the past experimental studies on the fracture energy obtained by the laboratory fracture energy tests using dam concrete of maximum aggregate size of 80 mm or more. In addition, considering the results obtained by the literature search, crack propagation analysis based on smeared crack model for an arch dam using three-dimensional FE model was conducted.

## 2 SUMMARY OF PREVIOUS TESTS ON FRACTURE ENERGY FOR DAM CONCRETE

A large number of experimental studies on the fracture behavior of concrete using relatively small aggregate have been conducted, but there are a few test cases of dam concrete using large aggregate. Literatures related to fracture energy tests satisfying the following conditions were gathered and organized.

1. Laboratory tests for dam concrete with maximum aggregate size of 80 mm or more were conducted.
2. Relatively large fracture energy more than about 300 N/m was obtained.

A summary of the literature search results is shown in Table 1. The meaning of the symbol concerning the specimen size in Table 1 is shown in Figure 1. The results in Table 1 are summarized in order from the oldest published date. Some fracture energy test methods were proposed including three point bending tests and wedge splitting tests, but only the results of wedge splitting tests met the above two conditions in the literature search in this paper.

He et al. (1992) conducted wedge splitting tests under the static and rapid loading conditions using specimens of maximum aggregate size of 76 mm. In the rapid test condition, time to peak loading was about 2.9 seconds. Fracture energy values were 152 and 1313 N/m for static and rapid loading conditions respectively and the ratio of the fracture energy in rapid test result to that in the static condition was about 8.6.

Trunk et al. (1998) conducted wedge splitting tests using specimens of maximum aggregate size of 125 mm. Specimen size was the largest and specimen age was the oldest in Table 1. Relatively large value of fracture energy of about 600 N/m was obtained by static loading test condition.

Table 1 . Summary of fracture energy tests by wedge splitting tests for dam concrete.

Author(s)	Maximum aggregate size	Compressive strength	Tensile strength	Specimen size of wedge splitting test (mm)				$H_2/d_{max}$	Fracture energy		Specimen age for fracture energy test
	$d_{max}$ (mm)	(N/mm <sup>2</sup> )	(N/mm <sup>2</sup> )	H <sub>1</sub>	W	D	H <sub>2</sub>		G <sub>F</sub> (N/m)		
He et al. (1992)	76	16.92 <sup>**2</sup>	2.00 <sup>**2</sup>	1820	1820	230	1366	5.94	static	152	55 days
									rapid <sup>**8</sup>	1313	
Trunk et al. (1998)	125	-	-	3200	3200	-	1600	12.8	static	about 600	More than 1 year
Horii et al. (2000)	150	34.1 <sup>**3</sup>	2.53 <sup>**3</sup>	1200	1200	450	600	4	static	317	-
	20	17.6 <sup>**4</sup>	1.84 <sup>**4</sup>	200	200	100	100	5	rapid <sup>**9</sup>	349	-
Zhao et al. (2008)	80	51.7 <sup>**5</sup>	-	1000	1000	500	500	6.25	static	about 660	1 year
Ishiguro (2014)	80 <sup>**1</sup>	26.9 <sup>**6</sup>	3.09 <sup>**6</sup>	315	350	200	260	3.25	static	411	more than 91 days
Guan et al. (2015)	150	29.37 <sup>**7</sup>	3.04 <sup>**7</sup>	2250	2250	450	1350	9	static	759	180 days

\*1: maximum aggregate size was 120 mm for mixing and specimens were prepared by wet screening using an 80 mm sieve, 2: specimen age is unknown, 3: specimen age is about 3 months, \*4: specimen age is about 1 month, 5: specimen age is 1 year, 6: specimen age is 91 days, 7: specimen age is 180 days, 8: time to peak loading (130kN) is about 2.9 seconds, 9: CMOD velocity is 12400 cm/minute.

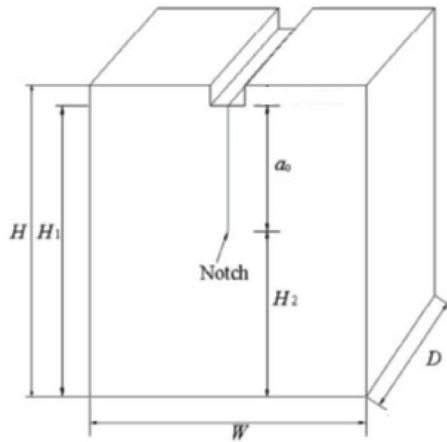


Figure 1. Outline of specimen used for wedge splitting tests.

Horii et al. (2000) conducted wedge splitting tests under the static conditions using specimens of maximum aggregate size of 150 mm and the fracture energy was 317 N/m. Horii et al. also conducted tests under the rapid loading conditions using specimens of maximum aggregate size of 20 mm and the fracture energy was 349 N/m. Horii et al proposed the following approximate expression on fracture energy by the results in static loading condition.

$$G_F = (0.79d_{max} + 80) \times (f_c/10)^{0.7} \quad (1)$$

where  $G_F$  = fracture energy (N/m);  $d_{max}$  = maximum aggregate size (mm); and  $f_c$  = compressive strength (N/mm<sup>2</sup>).

Zhao et al. (2008) conducted wedge splitting tests using specimens of maximum aggregate size of 80 mm. Fracture energy tests were conducted at the age of one year of specimens. Relatively large value of fracture energy of about 660 N/m was obtained for static loading test condition.

Ishiguro (2014) conducted wedge splitting tests using relatively small specimens. Concrete used for tests was mixed using maximum aggregate size of 120 mm and specimens (350 mm x 350 mm x 200 mm) were prepared by wet screening using an 80 mm sieve. Relatively large value of fracture energy of 411 N/m was obtained from static loading test condition.

Guan et al. (2015) conducted wedge splitting tests using relatively large specimens. Dam concrete mixed at an arch dam construction site was used. Maximum aggregate size was 150 mm and specimens were prepared by site-casting. Relatively large value of fracture energy of 759 N/m was obtained from static loading test condition. Guan et al proposed the following approximate expression on fracture energy by the test results.

$$G_F = (0.1616d_{max} + 1.0263) \times f_c \quad (2)$$

where  $G_F$  = fracture energy (N/m);  $d_{max}$  = maximum aggregate size (mm); and  $f_c$  = compressive strength (N/mm<sup>2</sup>).

Figure 2 shows fracture energies estimated by equations (1) and (2) when maximum aggregate size,  $d_{max}$ , is 150 mm. In Figure 2, the values of fracture energy are almost same when  $f_c$  is less than 10 N/mm<sup>2</sup>, but the difference becomes larger as  $f_c$  increases. One of the reasons of the difference between the values of fracture energy in Figure 2 was thought to be a relatively small value of  $H_2/d_{max}$  in the test conditions of Horii et al. (2000) in Table 1. Many papers indicate that the values of  $H_2/d_{max}$  are important to obtain stable values of fracture energy independent from the maximum aggregate size in the laboratory wedge splitting tests. The values of fracture energy increase almost linearly to  $H_2/d_{max}$  when  $H_2/d_{max}$  is small, but the

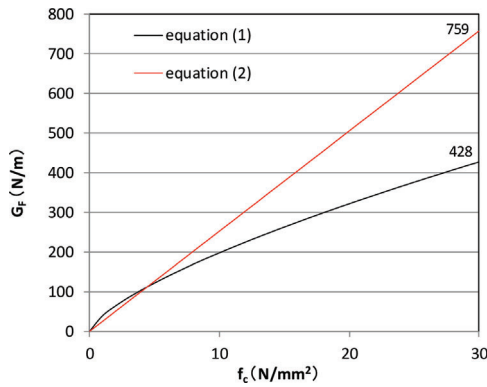


Figure 2. Relationship  $G_F$  and  $f_c$  of equations (1) and (2) in the case of  $d_{\max} = 150$  mm.

values of fracture energy become constant when  $H_2/d_{\max}$  is larger than a threshold value. Guan et al. (2015) pointed that the threshold value of  $H_2/d_{\max}$  was 6.

Based on the literature search results, three values of fracture energy were selected for crack propagation analysis to investigate the influences of the fracture energy on crack generation during earthquakes.

1.  $G_F = 428$  N/m obtained by the equation (1) when  $f_c = 30$  N/mm<sup>2</sup> and  $d_{\max} = 150$  mm shown in Figure 2. This value has sometimes been used for crack propagation analysis in Japan.
2.  $G_F = 759$  N/m obtained by the test conducted by Guan et al. (2015) in the static loading test condition in Table 1. This value is also obtained by the equation (2) when  $f_c = 30$  N/mm<sup>2</sup> and  $d_{\max} = 150$  mm shown in Figure 2.
3.  $G_F = 1313$  N/m obtained by the test conducted by He et al. (1992) in the rapid loading test condition in Table 1.

### 3 EFFECTS OF FRACTURE ENERGY ON CRACK PROPAGATION ANALYSIS FOR ARCH DAM

Embanking and impounding analysis were conducted to estimate initial stress. Then, crack propagation analyses based on the smeared crack model were conducted to evaluate crack distributions during earthquakes according to fracture energy.

#### 3.1 Analytical model

To investigate the influence of fracture energy on cracked area during earthquakes, crack propagation analysis based on the smeared crack model was carried out using a three-dimensional arch dam coupled model of dam body - foundation rock - reservoir (Figure 3). An arch dam model was used for study with a height and a water level of 105 and 93 meters, respectively. Reservoir was modeled by fluid elements and analyzed as a compressive fluid. Hexahedral elements with sides less than 1.5 m were used for dam body elements. The numbers of elements were 153,700, 70,448 and 149,392 for dam body, foundation rock and reservoir, respectively. The total number of elements was 373,540 for analysis. Transverse and peripheral joints were modeled using joint elements as shown in Figure 4, so that the opening and closing of the joint behavior can be considered in the analysis. The FEM software of ISCEF was used for analysis.

#### 3.2 Physical properties for analysis

Physical properties used for analysis are shown in Table 2. Unit weight and tensile strength were obtained by the laboratory tests for dam concrete of the model dam. Elastic modulus of

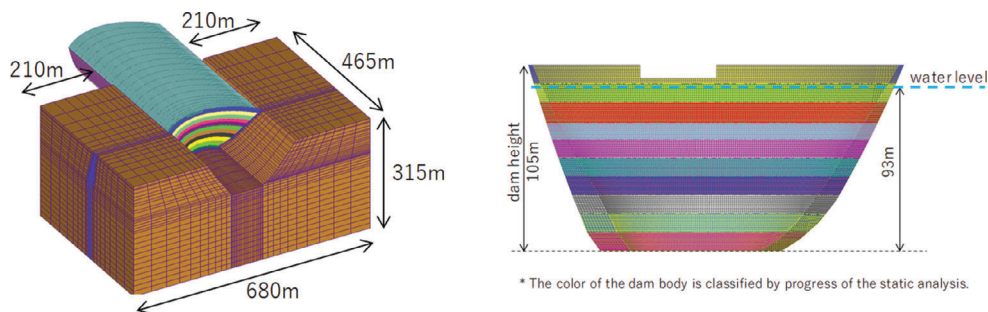


Figure 3. Entire analytical model (left) and downstream surface of dam body (right).

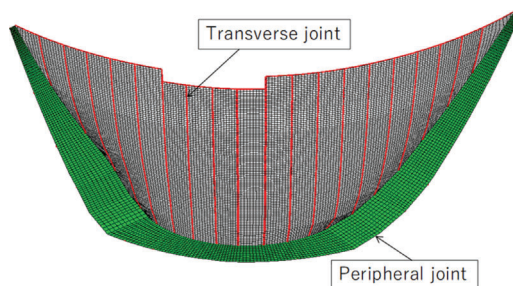


Figure 4. Transverse and peripheral joints.

Table 2. Physical properties for study.

	Unit weight (kN/m <sup>3</sup> )	Elastic modulus (N/mm <sup>2</sup> )	Poisson's ratio	Tensile strength (N/mm <sup>2</sup> )	Fracture energy (N/m)	Damping ratio (%)
dam body	24.5	45600	0.2	3.3	428, 759, 1313	5
foundation rock	26.5	32500	0.25	-	-	5
reservoir	9.8	Compressible fluid (c=1472m/s)				

dam body and foundation rock were estimated by the reproduction analysis using observed small seismic records of the model dam. Poisson's ratio and damping ratio of dam body and foundation rock were the values generally used in seismic analysis for arch dams. To investigate the effects of fracture energy on crack propagation, three values of fracture energy were selected based on the literature research described in Chapter 2. For tension softening curve of dam concrete for crack propagation analysis, linear function shown in Figure 5 was used.

Joint elements were used for the transverse and the peripheral joints so that the opening and closing of the joint behavior can be considered in the analysis. Physical properties for joint elements in Figure 6 were determined based on Nishiuchi et al. (2006) and Ariga et al. (2004).

### 3.3 Input motions

Figure 7 shows examples of acceleration time histories and acceleration response spectrum of input motions for three directions when the Peak Ground Acceleration (PGA) is 3 m/s<sup>2</sup> in the upstream - downstream (UD) direction. The original acceleration time history records were the record observed at the Kasho dam during the Western Tottori prefecture earthquake in

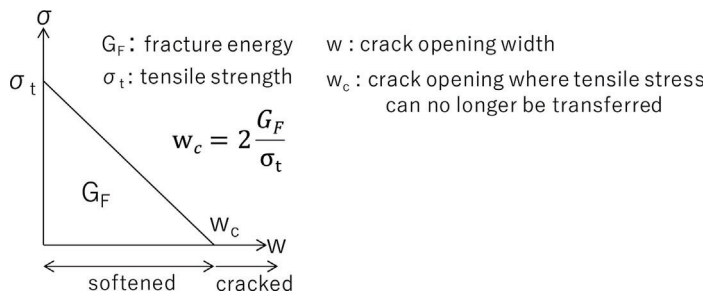


Figure 5. Tension softening curve used for study.

	Transverse joint element	Peripheral joint element
Axial modulus		
Shear modulus		
Damping ratio	1%	10%

Figure 6. Axial and shear modulus and damping ratio for joint elements.

2000 and the records were arranged for input motions by amplitude adjustment and spectrum fitting to the target acceleration and the target spectrum. Figure 7 also shows minimum acceleration response spectrum in Japanese guidelines (River bureau of MLIT, 2005), and the acceleration response spectrum of the input acceleration used for the analysis was set to conform to Japanese guidelines as shown in Figure 7. Three kinds of the PGA in the UD directions were used for analysis, 2, 2.5 and 3 m/s<sup>2</sup>, respectively. In order to shorten the time required for numerical analysis, acceleration time histories from 7 to 14 seconds with relatively large accelerations were used as shown in Figure 7.

### 3.4 Analytical results

Figures 8 - 10 show the results using input motions with the PGA of 2, 2.5 and 3 m/s<sup>2</sup> in the UD directions, respectively. In the figures, red element shows cracked area, and yellow element shows softened area where the tensile stress exceeds the tensile strength but crack is not generated in the element. Red joint shows that the joint element has opened.

Figure 8 shows the results of the PGA of 2 m/s<sup>2</sup> in the UD direction. Analysis of the case using the value of the fracture energy of 1313 N/m was not conducted. No cracked area or softened area were not confirmed in the upstream surface except elements near foundation

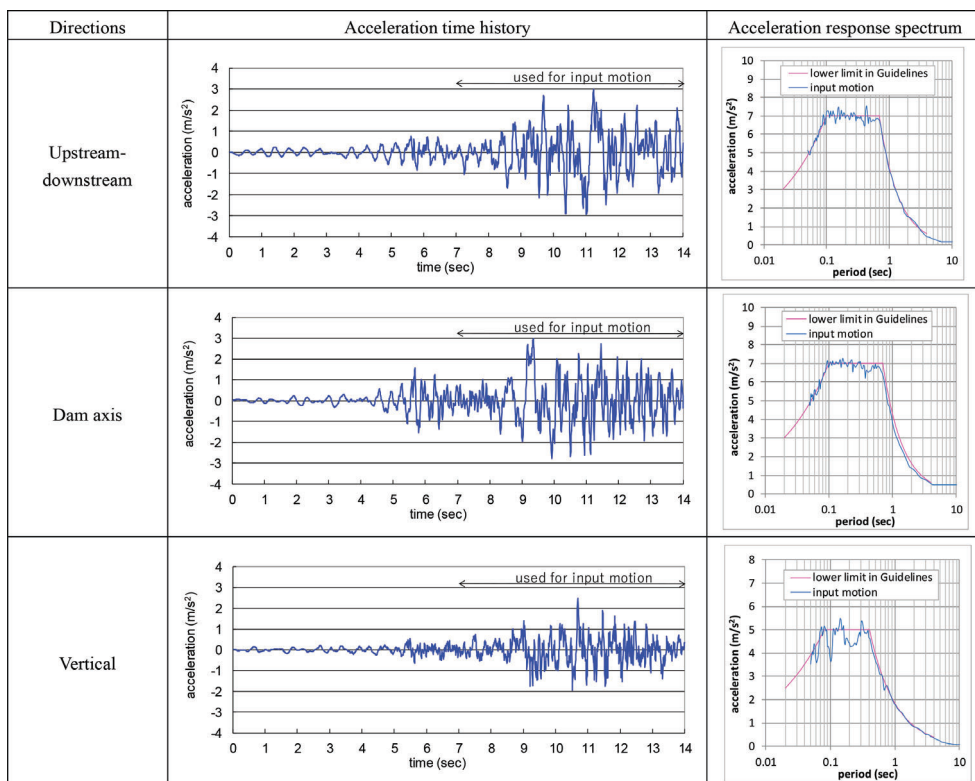
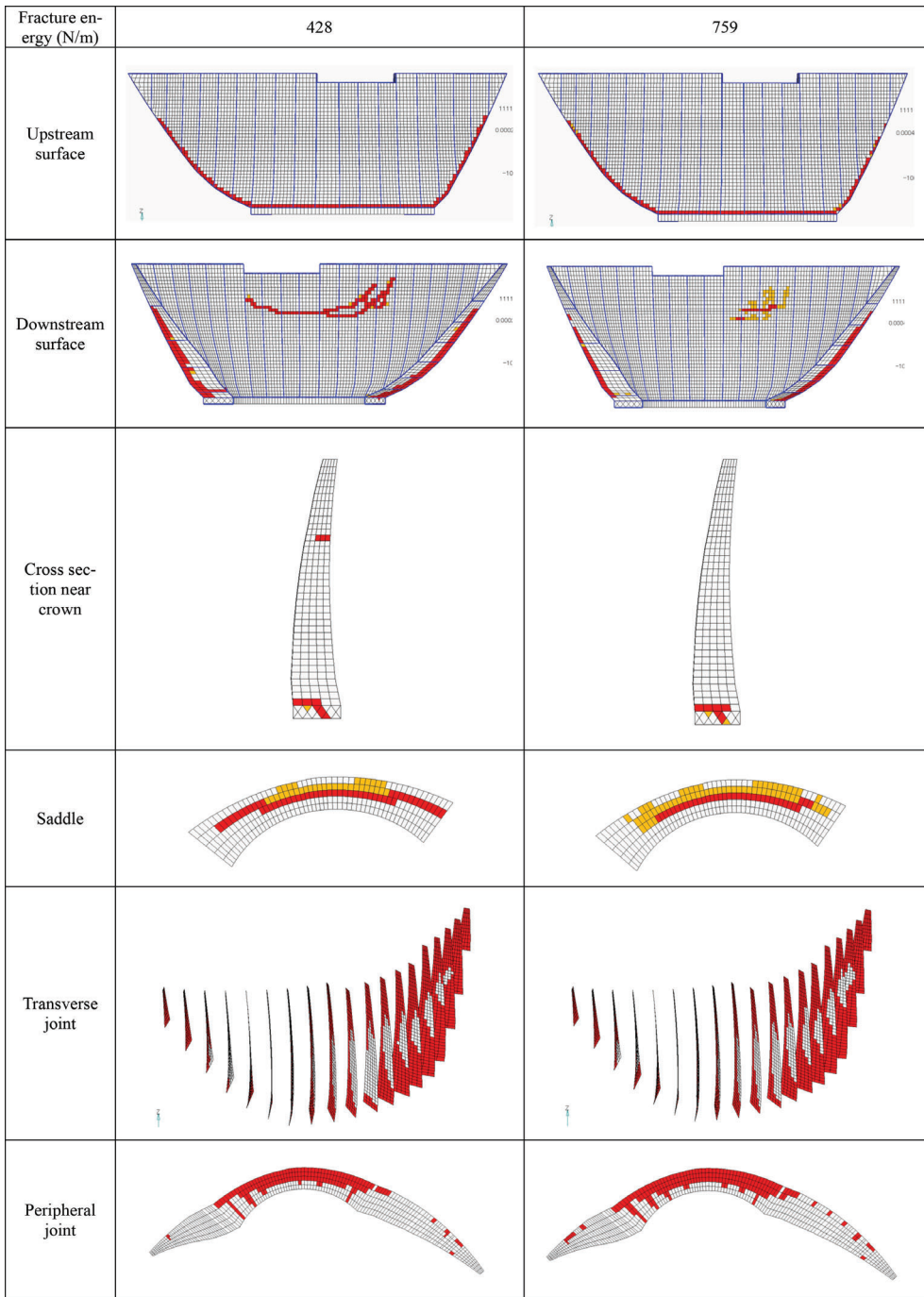


Figure 7. Acceleration time histories and acceleration response spectrum of input motions in the case of the maximum acceleration of  $3 \text{ m/s}^2$  in upstream-downstream direction.

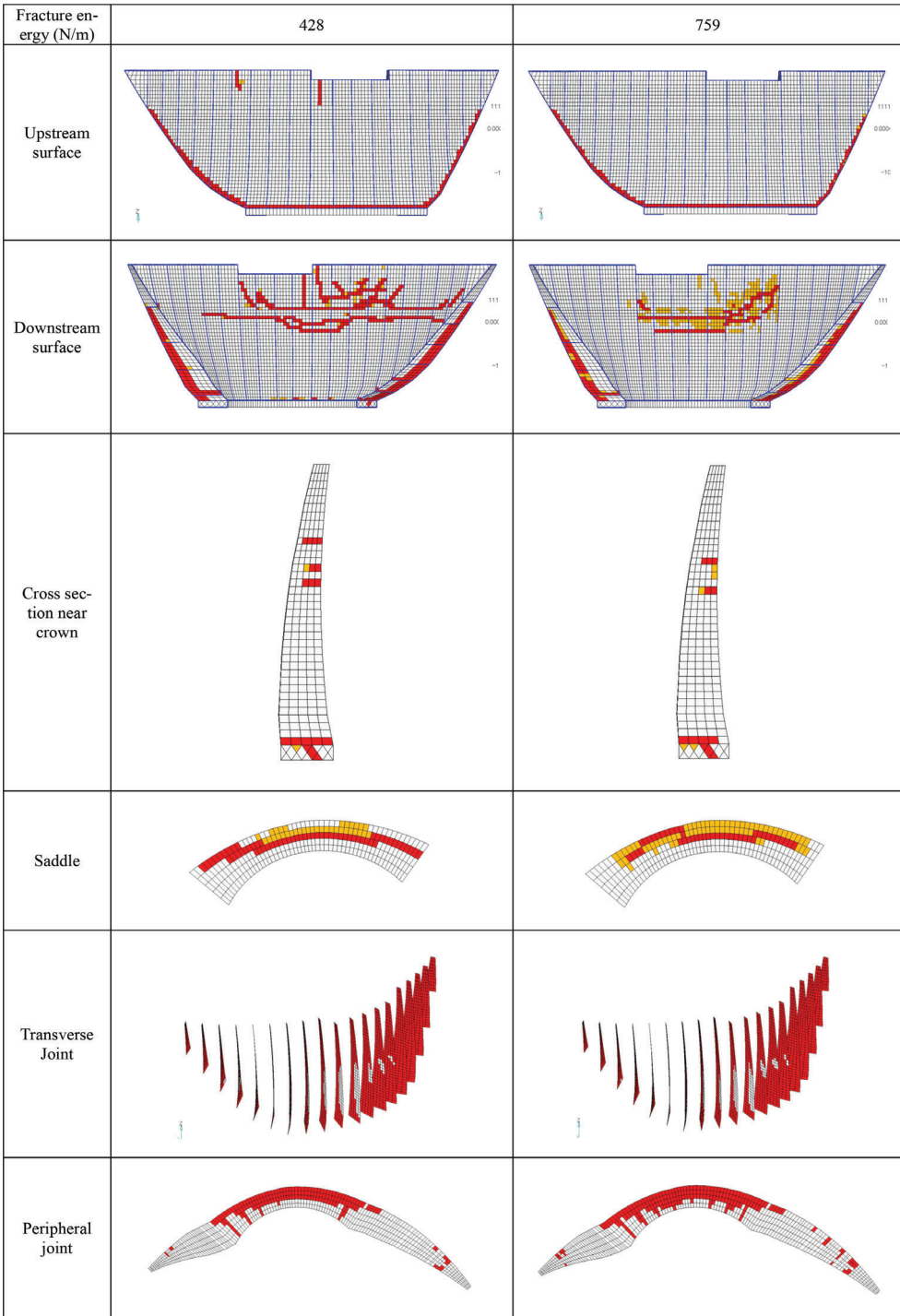
rock where stress concentration occurred. Horizontal continuous cracks were confirmed in the downstream surface in the case of the fracture energy of  $428 \text{ N/m}$ , but a few cracked elements were confirmed in the case of the fracture energy of  $759 \text{ N/m}$ . On the contrary, the number of softened elements in yellow in the case of the fracture energy of  $759 \text{ N/m}$  is greater than that in the case of the fracture energy of  $428 \text{ N/m}$ . Almost no softened elements were confirmed in the downstream surface in the case of the fracture energy of  $428 \text{ N/m}$ , because tensile stress was released by the cracked elements. Many joint elements of transverse joints had opened and it was thought that joint opening contributed to less cracked elements of dam body. Large differences of opened joints according to the fracture energy cases of  $428$  and  $759 \text{ N/m}$  cannot be found.

Figure 9 shows the results of the PGA of  $2.5 \text{ m/s}^2$  in the UD direction. Analysis of the case using the value of the fracture energy of  $1313 \text{ N/m}$  was not conducted. Small vertical cracked area in red was confirmed in the upstream surface in the case of the fracture energy of  $428 \text{ N/m}$ , but no cracked area in the case of the fracture energy of  $759 \text{ N/m}$  except elements near foundation rock where stress concentration occurred. Two or three horizontal continuous cracks were confirmed in the downstream surface in the case of the fracture energy of  $428 \text{ N/m}$ , but less cracked elements were confirmed in the case of the fracture energy of  $759 \text{ N/m}$  than those in the case of  $428 \text{ N/m}$ . On the contrary, the number of softened elements in yellow in the case of the fracture energy of  $759 \text{ N/m}$  is greater than that in the case of the fracture energy of  $428 \text{ N/m}$ . Only a few softened elements were confirmed in the downstream surface in the case of the fracture energy of  $428 \text{ N/m}$ , because tensile stress was released by the cracked elements. More joint elements of transverse joints had opened than in the Figure 8. Large differences of opened joints between the fracture energy cases of  $428$  and  $759 \text{ N/m}$  cannot be found.



\*Red element : cracked area. Yellow element : softened area. Red joint : opened joint.

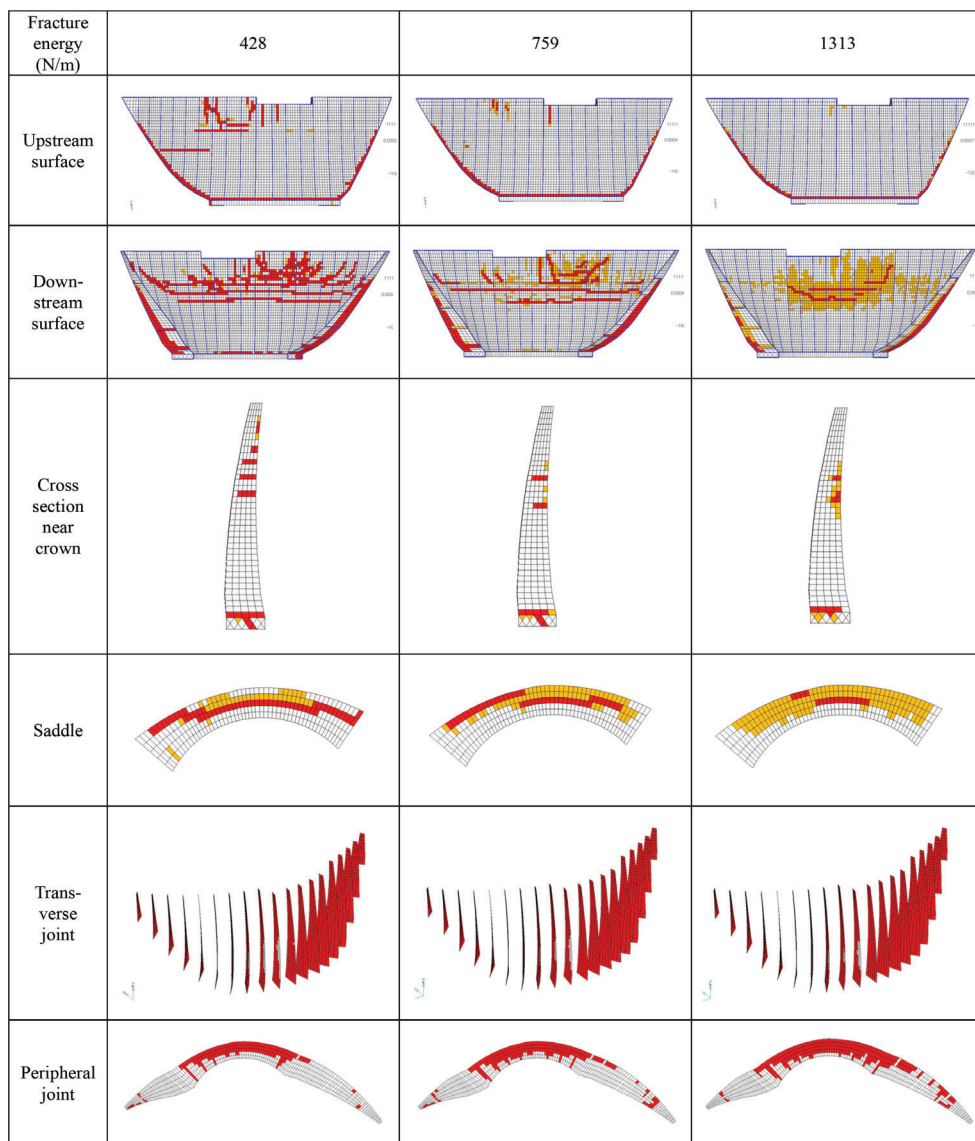
Figure 8. Crack distributions and joint openings in the case of  $PGA = 2 \text{ m/s}^2$ . \*Red element: cracked area. Yellow element: softened area. Red joint: opened joint.



\*Red element : cracked area. Yellow element : softened area. Red joint : opened joint.

Figure 9. Crack distributions and joint openings in the case of  $PGA = 2.5 \text{ m/s}^2$ . \*Red element: cracked area. Yellow element: softened area. Red joint: opened joint.

Figure 10 shows the results of the PGA of  $3 \text{ m/s}^2$  in the UD direction. Vertical and horizontal cracked area in red was confirmed in the upstream surface in the case of the fracture energy of  $428 \text{ N/m}$ , but no cracked area in the case of the fracture energy of  $1313 \text{ N/m}$  except elements near foundation rock where stress concentration occurred. More cracks were confirmed in the downstream surface than in the Figure 9 because of increase of input accelerations. As fracture energy increased, cracked area in the downstream surface became smaller and cracks were localized, but softened area became larger. Softened area in the downstream surface was small in the case of the fracture energy of  $428$ , but softened area was larger than cracked area in the case of the fracture energy of  $1313 \text{ N/m}$ , because tensile stress was transferred through the softened elements. More joint elements of transverse joints had opened than in the Figure 9. Large differences of opened transverse joints between the fracture energy



\*Red element : cracked element. Yellow element : softened element. Red joint : opened joint.

Figure 10. Crack distributions and joint openings in the case of  $\text{PGA} = 3 \text{ m/s}^2$ . \*Red element: cracked element. Yellow element: softened element. Red joint: opened joint.

cases of 428, 759 and 1313 N/m cannot be found. Opened peripheral joints slightly increased as fracture energy increased.

#### 4 CONCLUSIONS

To investigate the effects of fracture energy on crack propagation in arch dam during large earthquake, literature search was conducted to evaluate fracture energy of dam concrete and crack propagation analysis was also conducted. The following conclusions are obtained.

1. We investigated the past experimental studies on the fracture energy laboratory tests. Literatures related to fracture energy tests satisfying the following conditions were gathered. First condition was that laboratory tests for dam concrete with maximum aggregate size of 80 mm or more were conducted. Second condition was that relatively large fracture energy more than about 300 N/m was obtained. We found six papers satisfying the conditions and summarized test conditions and test results. Relatively large values of fracture energy were obtained by the tests in the papers and the maximum values were 759 and 1313 N/m by static and rapid loading conditions, respectively. These values are only the results of the literature search in this paper, so it is possible larger fracture energy has been obtained in other papers.
2. Crack propagation analyses base on smeared crack model for an arch dam with a height of 105 m using three-dimensional FE model were conducted. Joints were modeled by the joint elements to reproduce nonlinear behavior of the joints of the arch dam. The input values of the fracture energy were determined based on the literature search. Three acceleration time histories with maximum accelerations of 2, 2.5 and 3 m/s<sup>2</sup> were prepared and used for input motions. The numerical results showed that the fracture energy had important influences on crack distributions. As fracture energy increased, cracked area in dam body became smaller and cracks were localized, but softened area became larger.

We think that it is possible that the value of the fracture energy of the dam concrete used in arch dams is greater than the values shown in Table 1, because the compressive strengths of some arch dams in Japan are larger than those in Table 1. We are now planning experiments on fracture energy test by wedge splitting tests using large specimens and dam concrete of maximum aggregate size of 150 mm and maximum compression strength of 65 N/mm<sup>2</sup>.

#### REFERENCES

- Ariga, Y., Cao Z. and Watanabe, H. 2004. Study on 3-D dynamic analysis of arch dam against strong earthquake motion considering discontinuous behavior of joints. *Journal of Japan Society of Civil Engineers*: 759, 53-67. (in Japanese)
- Guan, J., Li, Q., Wu, Z., Zhao, S., Dong, W. and Zhou, S. 2015. Minimum specimen size for fracture parameters of site-casting dam concrete. *Construction and Building Materials*: 93, 973-982.
- He, S., Plesha, M., Rowlands, R. and Bezant, Z. 1992. Fracture energy tests of dam concrete with rate and size effects. *Dam Engineering*: III, 139-159.
- Horii, H., Uchita, Y., Kashiwayanagi, M., Kimata, H. and Okada, T. 2000. Study on tensile softening characteristics for evaluating concrete dam strength. *Electric Power Civil Engineering*: 286, 113-119. (in Japanese)
- ISCEF. <http://www.century-techno.co.jp/products/>.
- Ishiguro, S. 2014. Wedge splitting tests of concrete with large coarse aggregate size. *Proceedings of the Japan Concrete Institute*: 36, 1, 352-357. (in Japanese)
- Nishiuchi, T. and Sakata, K. 2006. Investigation on static behavior of existing arch dams using finite element method considering nonlinear behavior of transverse joints. *Journal of Japan Society of Civil Engineers*: 62, 4, 672-688. (in Japanese)
- River Bureau, Ministry Land, Infrastructure, Transport and Tourism (MLIT), 2005. *Guidelines for seismic performance evaluation of dams during large earthquakes (draft)*.
- Trunk, B. and Wittmann, F.H. 1998. Experimental Investigation into the Size Dependence of Fracture Mechanics Parameters. *FraMCoS-3*: 1937-1948. Gifu.
- Zhao, Z., Kwon, S. and Shah, S. 2008. Effect of specimen size on fracture energy and softening curve of concrete: Part I. Experiments and fracture energy. *Cement and Concrete Research*: 38, 1049-1060.